

Wearable Sensor Network for Human Locomotion Data Capture

Joana Lobo†, Joana Silva‡, Márcia Vagos§, Nádia Silva¶, Nuno SousaØ, Sílvia Bessa‡

Abstract—Gait is a complex sequence of neuromuscular events that has a very important role on daily life. Injuries or diseases can affect human motion and physicians still struggle to diagnose gait disorders since the existent systems for gait analysis are functionally limited. A novel gait analysis system, ProLimb, is then suggested. This project encompasses a wearable and portable system with textile based sensors, connected in a body area network, providing an experimental solution for gait analysis, extracting inertial and electromyographic integrated data on the lower limbs. We built, tested and evaluated a functional prototype. Textile electrodes have showed to be a solution with potential for long-term gait monitoring. Further optimization of the ProLimb system is also discussed.

Index Terms—Gait Analysis, Kinematics, Mesh Network Topology, Body Area Network, Wearable Sensors, Textile Electrodes, Electromiography, IMU;

I. INTRODUCTION

GAIT is the sequence of movements where the body travels supported by leg motion. This process can be affected by motor-sensory dysfunction, inadequate neuromuscular responses, musculoskeletal impairments or decreased cognition (inability to anticipate or adapt to postural needs) [1]. Despite the increasing number of conditions that affect gait movement, where population aging is the major contributor along with Parkinsons disease and stroke, physicians still struggle to diagnose gait disorders by analyzing patient motion [2]. Gait is a complex process and the existent systems for gait analysis are still functionally limited, lacking practical approaches for gait assessment without biasing results.

In this sense, gait analysis is a diagnosis method that records human kinematics and dynamics during a certain gait movement, providing quantitative data to analyze and diagnose movement disorders [3]. When combined with electromyography (EMG) records, technologies for gait analysis are appealing as diagnostic and inspection tools. Gait analysis systems are commonly used by athletes and people suffering from diseases or injuries conditioning gait. They assess pathology or injuries severity, monitor patients progress either in the presence or absence of an intervention, and predict better treatments [3]

In gait analysis, clinicians are more interested in evaluating a set of parameters than the raw data itself. For that reason,

data processing tools should address the extraction and quantification of gait parameters from inertial and surface EMG signals. Two classes of spatio-temporal features are commonly extracted from data: kinetic and kinematic [4], [5]. Kinetic variables include: mean gait velocity, stride length and width, step length, step frequency-cadence (steps per minute), stance, swing and double stance percentage with respect to stride phase, maximal values of the hip and ankle joint moments and powers (plantarflexion, extension and flexion moments). The main kinematic variables are: range of amplitude of each lower limb joint (hip, knee, ankle), calculated as the difference between the minimum and maximum flexion angles in the whole stride and in the stance and swing phase, pelvic orientation in the frontal plane.

In the presence of these values, gait normality is generally assessed by comparing them into standard values. Elderly people as well as patients suffering from movement disorders derived from neurological diseases, such as Parkinson Disease (PD), are often affected by motor disability with reduced range of motion. It has been reported that PD patients present typical walking pattern with reduced velocity, increased stance phase and shorter stride length, with decreased amplitude of the lower limb segment [4]. The analysis of the aforementioned parameters allows not only the overall evaluation of gait disability, but also the comparison of motor performance of both body sides. The additional data from EMG further improves these tasks, and it might be crucial to infer patient's conditions. For instance, kinematics records can be compared to EMG plots to find out if joint angular motion can explain EMG or EMG can explain angular motion. Besides, EMG signals are affected by the velocity of gait [6]. Considering the case of PD as an example, EMG signals with lower amplitudes would be associated with the lower gait's velocity of these patients. Although data bases about EMG and inertial sensors patterns are limited, some standard values are already stated and deviations from these are even associated with specific diseases [7].

At the present time, gait analysis is commonly performed in laboratory or physicians office. Manual observational inspection, image acquisition or sensor based data acquisition systems for kinematics detection, force systems or pressure mapping for dynamics measurement are used as well as surface EMG (sEMG) for determining muscle activity. However, these systems can be expensive and in general they are difficult to use. They are uncomfortable for the patient, are time consuming and can require high levels of expertise. These features hamper the use of gait analysis in several rehabilitation areas. For instance, gait analysis has potential as

FEUP- MIB - Eng. Biomedica

†bio08036@fe.up.pt

‡bio08058@fe.up.pt

§bio08075@fe.up.pt

¶bio08002@fe.up.pt

Øbio08062@fe.up.pt

‡bio07040@fe.up.pt

a monitoring system during rehabilitation of injured athletes. Their main goal is to recover full gait function in a short-time and without increasing the risk of a relapse and gait analysis could help by providing means to assess the real physical condition and adjust treatments. Nevertheless, the lack of a practical method to evaluate gait in a lab free environment is the main obstacle to its use in the field of sport's medicine. Monitoring in sports is still based on medical manual and visual observation, considerable follow up of training images and athlete opinion related with pain. Based on that, gait analysis systems and procedures should preferably include real and continuous time monitoring, being inexpensive, easy-to-use and widely available [8]. In addition, gait analyses provided by current systems do not reflect motor function under real-life conditions [8]. There is a need for a low cost device that can provide quantitative and reproducible results, as well as monitor gait over long periods of time. In particular, gait analyses of patients with Parkinsons disease would be greatly enhanced by studying gait outside of a limited motion lab area [8], as for it happens for sportive follow up.

To address these problems, a novel gait analysis system, ProLimb, is being developed. ProLimb is a comfortable, wearable system for gait analysis and monitoring. The core technology is an electronic instrument to capture objective data on human motion combined with a textile support (stockings or pantyhose) making the product practical and non-invasive. The conjugation of these two components makes the infrastructure portable and allows performing the analysis in and outside of a laboratory environment, for prolonged periods of time, monitoring typical movement activities under everyday living conditions. For this purpose, ProLimb comprises eight sensor nodes (SN) disposed in a mesh topology, containing accelerometers, gyroscopes and textile sEMG sensors for capturing lower limbs kinematics (namely linear and angular movement) and surface electromyographic signals, respectively. Four SN are placed per leg, each one monitoring a different target muscle, namely the Biceps Femoris, the Rectus Femoris, the Tibialis anterior and the Gastrocnemius. The acquired data is transmitted via wire to a central processing module (CPM) attached to the patients belt. In the present study, we were asked to test functional prototypes and actively participate in the miniaturization of the SN, envisaging the wearable and longterm analysis purposes of the ProLimb system. Suggestions of alterations to the initial prototype would also be welcomed.

II. METHODS

A. Functional prototype assembly and testing

To implement the described Body Area Network (BAN), conductive yarn was used to put together the network of SN and sEMG electrodes and connect it to the CPM [9], [10]. The conductive yarn is made of multifilament polyamide and elastane fabric. This material is widely used in textile industry for being very comfortable, easy to knit into cloth and for its elastic properties. The yarn is coated with a thin silver layer to render it conductive (with a mean mass resistance of roughly 4R/cm, higher than that of copper wire). Other possibilities

were available, namely silver covered pure polyamide or polyester yarn, stainless steel covered yarn, or even pure stainless steel yarn. In this project only silver/polyamide/elastane yarn was used. The yarn is embedded in the cloth, onto the basic fabric, during the fabrication process in the Textile Engineering Department of Minho University [11] and using a technique to embody textile electrodes (TE), connections and the reference electrode (RE) in the stockings. We are using a LIR2450 Lithium Battery as power supply. In an initial stage, the BAN of the prototype was implemented only on the right leg with 4 SN with a data acquisition rate of 73,6 Kbits/s, according to the following architecture (Figure 1):

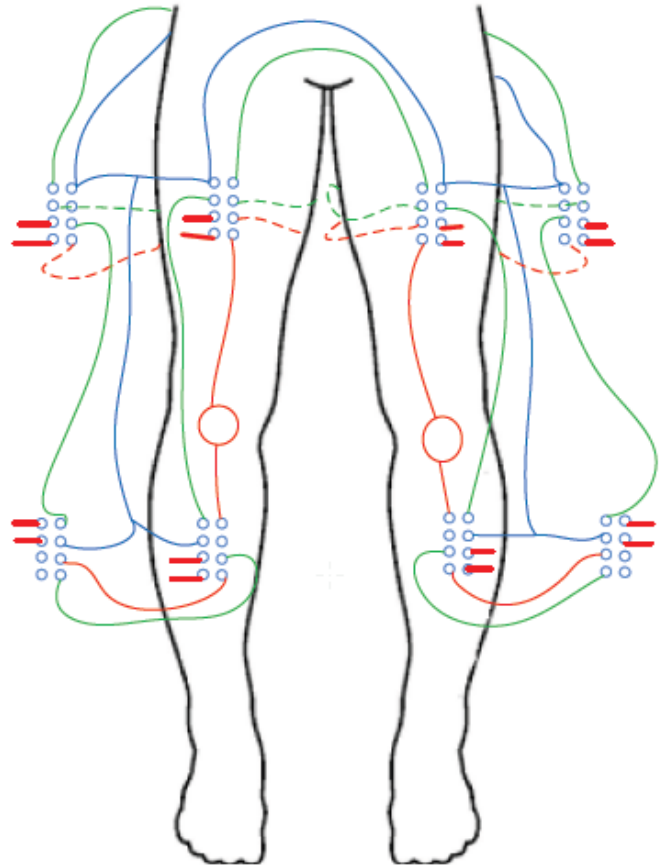


Fig. 1. Connections and Nodes and connections

- 2 SN with inertial measurement unit (IMU) and sEMG (4 + 4 signals) in the anterior upper and lower limb;
- 2 SN only with sEMG (2 + 2 signals) in the posterior upper and lower limb.

Two different topologies for the Right-Leg Drive (RLD) were considered:

- Connect all RE signals independently for the reference electrode in the knee;
- Connect all RE signals in a single point, and link this point to the RE.

The second topology was adopted since it is easier to implement and also because it allows for noise coupling of the signals and minimization of wiring length, resulting in

possibly improved signal to noise ratio. A functional prototype (Fig.2) has been prepared with the TE and circuit leads stitched upon the leggings to test the optimal configuration of the circuit, taking into account the minimization of lead length and interferences. On the first version of this prototype, conductive lines were weaved in separate pieces of cloth and then manually knitted on the top of the stockings. This knitting process is time-consuming and not practical. Sensor Nodes were then mounted on the leggings using metal attaches which simultaneously provide anchorage and electric contact. To fix the attaches to the SN, two possibilities were considered:

- Gluing a patch of cloth to the backside of the SN board and stitching attaches to this intermediate support. The inputs and output on the top side of the SN would be extended to the back and soldered to the attaches.
- Building new PCBs with attaches directly soldered onto it, so that no intermediate support would be necessary. This possibility would require that each SN had to be unique with different correspondence between attaches and connectors, since circuit configuration is also different around each SN in the stockings. Nevertheless, this was the selected option. A scheme of the connections between the circuitry and attaches is shown in Figure 1

Two sets of preliminary tests were performed, and the recorded signals were analyzed later with MatLab. Testing was performed envisioning the comparison of the signals acquired with both TE and conventional electrodes (CE). All the tests were performed by a healthy young female with no history of gait disturbances. Data was collected for both TE and CE placed on the right leg of the volunteer, according to the following segments:

- *Segment a:* Maximum voluntary contraction full contraction of leg muscles during 4 seconds, with the foot on the ground and without movement;
- *Segment b:* Flexion in two steps knee flexion to the back and knee extension;
- *Segment c:* Flexion in four steps hip and knee flexion to the front, knee extension, knee flexion and return to initial position;
- *Segment d:* Flexion in six steps continuous movement of segment c followed by segment b;
- *Segment e:* Walking - Stand (5s), walk (12 steps) and remain still (5s);
- *Segment f:* Running - Stand (5s); run (12 steps) and remain still (5s).

An image of both CE and TE during the tests is presented on figure 2 To ensure correspondence of signals and acquisition in the same conditions, the two sets of signals (from CE and TE) should have been measured simultaneously with both sets of electrodes placed on the same muscles, but far enough to guarantee that overlapping and signal interference would not occur. For that purpose, additional holes near the TE would have been necessary to allow the introduction of CE beneath the stockings, and an extra set of acquisition and SN modules were necessary. As the necessary extra material was not available and the simultaneous usage of both sets of electrodes presented great discomfort and constraint to the

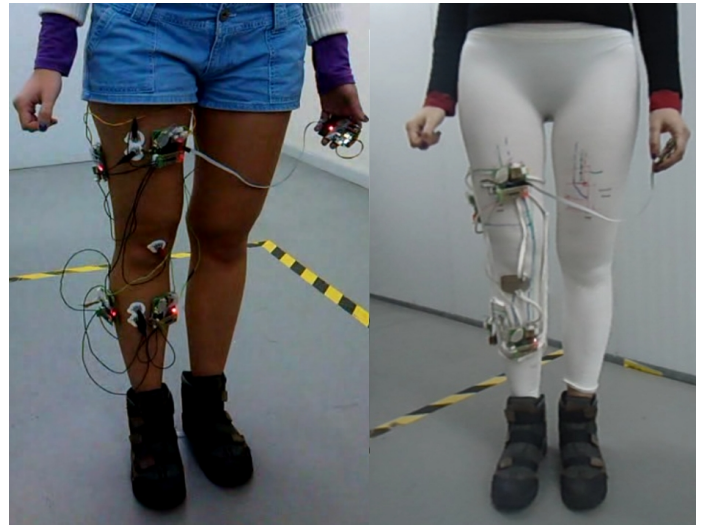


Fig. 2. Conventional Electrodes (left) and textil electrodes (right) prototypes

volunteer, CE and TE data was obtained in different and thus independent assays. This will limit signal comparison and decrease the reliability of the conclusions that can be extracted from these data.

B. Signal Analysis

The initial approach for the data analysis envisioned the following processing steps: temporal alignment of the signals coming from different SN, EMG signal processing including signal rectification, low pass filtering and IMU signal processing.

1) *Processing:* To identify locomotion patterns, the data acquired with CE and TE was filtered to remove the offset and noise. The offset was removed by an average filter, which was applied in the EMG and inertial signals acquired with CE and TE. In accordance with literature, EMG signals were filtered for noise reduction with a bandpass filter, to remove the baseline and very high frequency noise. Some authors employ a low cutoff frequency for the band pass of 100Hz to remove the 50Hz nearly ubiquitous noise, however this approach lead to some signal loss. Although in the literature the authors diverge in low cutoff frequency, the higher cutoff frequency usually is near the 500Hz. For this work it was designed a low-pass filter with cut-off of 500Hz, since the baseline was already removed by the average filter and the removal of some low frequencies could lead to some signal loss [12], [13]. In addition, a root mean square filter (RMS) filter was applied in EMG signals to obtain a better definition of peaks contraction. This approach is normally used for this type of signals. To reduce the noise in the inertial signals, a common low-pass filtering approach was applied [14], [15]. Therefore, a low pass filter was applied with a cutoff frequency of 200Hz.

2) Activity Profiles identification:

- One Sensor

For the identification of patterns present from one sensor in a certain test, a signal alignment approach was performed. Initially, the inertial signals were divided by their higher peak

to normalize amplitude. The alignment was performed using cross-correlation between acceleration and gyroscope signals, and the alignment information was used for the following steps of pattern identification. Afterwards, EMG signal was resampled and aligned with the resulting information. Resample was needed since the number of samples per minute in EMG was considerably higher than the sampling frequency from inertial sensors. The alignment was carried with the same approach used for inertial signals and the amplitude normalization was also need before this step.

3) *Multiple signal alignment*: Fruit of several delays of unknow (albeit estimable) nature there is a desynchronism present in the captured data. Let's assume that the sampling rates are dependable upon, managing this the desynchronism is of a purely delay nature. There are timestamps in the samples but even so the data doesn't align all that well. Hence came the necessity, for applications where classifiers of posture and activity, or Inverse Kinematics might be employed, having all the signals share a common time reference is of importance, so the challenge of making multiple signals synchronous came to light.

The available signals are as follows, accelerometers, gyroscopes, and Electromyographs. Let's assume that Accelerometers are aligned with their respective gyroscopes, (since they originate in the same physical IMU module), but the IMU bundle (accelerometers plus gyroscopes) is not aligned with the EMG signal, even from the same module, and different modules are disaligned amongst themselves.

To establish a common time frame we took advantage of the movements of the lower limb which most often affect both articulate pieces. Modelling the lower limb as two rigid bodies with an articulation, we have two sensor nodes in the calf and two in the thigh. It can be assumed that some of the movements which affect the calf will also affect the thigh, which is to say, there will be plenty of "coincidences" in the IMU signals between the lower and higher part of the leg. Those coincidences will allow for us to align the upper modules with the lower ones, since they are likely to show the best alignment when those parts which are indeed present in both signals overlap in the alignment algorithm.

The alignment of two time varying signals can be performed using by estimating the delay between the two which the maximum of the convolution between both. When such happens it means the overlapping areas are at a maximum. In order to maximize the performance of this method we apply a moving average real time remover to remove the baseline and settle the signal at 0, allowing us to overlap the activity in the signal. When performing this alignment between signals which aren't exactly equal, which in fact posse each eigen clusters which are not mutually occurring it is best to ignore the form, so the entire signals are rectified and passed through a smoothing kernel which is convoluted to yeald a low pass like function. This chain of processing is typical for emg, but is used as well in IMU for the sense of highlighting 'activity' zones, allowing for them to be aligned instead of focusing on peak alignment to increase the robustness of the method against isolated signal artifacts.

Using appropriate pre-filtering and resampling the 50sps sig-

nals of the IMUs to the EMGs 1Ksps we can align the EMG signals with the Inertial ones based on the assumption that contraction originates movement, so regions of emg activity will correspond to regions of movement.

When comparing multiple signals, such as in this case in which there are four nodes, the problem gets more complicated as there might (and very probably will) be mismatches in the *global alignment*. The problem rises when several routes of alignment don't yield the same delays: comparing signals A, B , and C which are not aligned but to whom we apply the Inter Signal Alignment methods resulting in the identified delays $d_{A,B}, d_{A,C}, d_{B,C}$ now if the estimated delays were perfect we could say:

$$d_{A,C} = d_{A,B} + d_{B,C} \quad (1)$$

Note that these delays can be positive, meaning B is delayed $d_{A,B}$ time in respect to A if positive, and vice versa if negative, thus equation 1 is valid for all cases that the delays are perfectly estimated. In all likelihood however it will happen that $d_{A,C} \neq d_{A,B} + d_{B,C}$, suppose B is delayed 40ms to A and C 70ms to A, yet the algorithm finds C delayed 80ms instead of 70ms when directly measuring the delay between B and C. To answer these multiple paths through which delays might be indirectly estimated we devised an approach which takes into account all measured delays and finds an optimal concordant solution of delays, which takes into account the information from all alignments to generate the global alignment and thus the best delays for each of the signals.

Given signals s_1, s_2, \dots, s_N each composed of L_i samples, $s_1 = [s_1(0)s_1(1)s_1(2)\dots s_1(L_1)]$ and knowing that they amongst themselves have estimatives delay $d_{i,j}$ which are zero for the alignment of the signal against itself, we can construct a global delay matrix:

$$D = \begin{pmatrix} d_{1,1} & d_{1,2} & \dots & d_{1,N} \\ d_{2,1} & d_{2,2} & \dots & d_{2,N} \\ \vdots & \vdots & \ddots & \vdots \\ d_{N,1} & d_{N,2} & \dots & d_{N,N} \end{pmatrix} \quad (2)$$

It is expected that the matrix shows negative symmetry, meaning that $d_{1,2} = -d_{2,1}$. In matrix D we have in each line how one signal is directly aligned to each of the others, and if we were to find the minimum at each row and delayed the signal by that value (for instance signal 1 has minimum -4 in row 1 that means if we cut 4 samples, seconds, ms... from the beginning of the signal he would be in the global time frame).

We haven't yet the information about the alternative paths. If we want to second guess the estimative $d_{i,j}$ we must look at all paths that go from i to j without repeating values.

Consider $N = 4$, the available paths to form the connection 1, 2 are $[(1, 2)]$ obviously, plus the connections by reference to a intermediate signal : $[(1, 3), (3, 2)], [(1, 4), (4, 2)]$ and to all signals $[(1, 3), (3, 4), (4, 2)], [(1, 4), (4, 3), (3, 2)]$, consider the matrix D .

$$D = \begin{pmatrix} d_{1,1} & d_{1,2} & d_{1,3} & d_{1,4} \\ d_{2,1} & d_{2,2} & d_{2,3} & d_{2,4} \\ d_{3,1} & d_{3,2} & d_{3,3} & d_{3,4} \\ d_{4,1} & d_{4,2} & d_{4,3} & d_{4,4} \end{pmatrix} \quad (3)$$

If we're trying to create paths from 1 there is no interest in including this column in because all it's members end in 1, meaning they end at the the beggining of the route, so we take that column out. Since we're trying to get to 2 there is no point in including row 2 because all of it's members depart from two, and after reaching 2 we needn't go anywhere else. So, from the remotion of this line and column we get the matrix:

$$D_{1,2} = \begin{pmatrix} d_{1,2} & d_{1,3} & d_{1,4} \\ d_{3,2} & d_{3,3} & d_{3,4} \\ d_{4,2} & d_{4,3} & d_{4,4} \end{pmatrix} \quad (4)$$

And in this matrix we can find all the combinations which result in a path from 1 to 2 , in other words the sequence of delays which estimate the delay from 2 to 1. This can be done by summing the diagonals and the secondary diagoonals of the matrix:

$$d_{1,2} = d_{1,2} + d_{3,3} + d_{4,4} \quad (5)$$

$$d_{1,2} = d_{1,3} + d_{3,4} + d_{4,2} \quad (6)$$

$$d_{1,2} = d_{1,4} + d_{4,3} + d_{3,2} \quad (7)$$

$$d_{1,2} = d_{1,4} + d_{3,3} + d_{4,2} \quad (8)$$

$$d_{1,2} = d_{1,3} + d_{3,2} + d_{4,4} \quad (9)$$

If we remove the term $d_{i,i}$ because it is equal to zero (the delay between a signal and itself) we have all the combinations earlier mentioned. By averaging all these values we can produce an estimate of the alignment with all possible alignments routes being accounted for. So when we produce the matrix $D_{i,j}$ resultant of the supression of the row j and column i and sum its diagonals and secondary diagonals and average we can get the matrix:

$$D_{Avg} = \begin{pmatrix} |D_{1,1}|* & |D_{1,2}|* & \cdots & |D_{1,N}|* \\ |D_{2,1}|* & |D_{2,2}|* & \cdots & |D_{2,N}|* \\ \vdots & \vdots & \ddots & \vdots \\ |D_{N,1}|* & |D_{N,2}|* & \cdots & |D_{N,N}|* \end{pmatrix} \quad (10)$$

And from the each line we may extract the actual delay we have to apply to each signal to have everything properly aligned with all alignments accounted for:

$$d_i = \min(D_{Avg,i}) \quad (11)$$

4) *Signal to Noise Ratio*: An important issue to investigate concerning the functional prototype implementation is if there were significant differences between EMG signals acquired with CE and acquired with TE. As described in the previous section, two sets of tests were performed: one using the SNs attached to the limbs with adhesive tape and the CE placed under the respective muscles; and another test was performed using the pantyhose that incorporated the TE. Since the CE and TE data was obtained in different and thus independent assays, SNR was used to compare the signals acquired with both TE and CE.

C. Miniaturization of the SN

In order to comply with the requirements regarding size and energy consumption, the sensor nodes had to be miniaturized. For this purpose, the design of the main-board of the SN and the sEMG Analog Front-End (AFE) was adapted to fit in a 3x3 cm PCB. The choice of this size was driven by the intention of making the SN as small and lightweight as possible for better integration in the garment. Moreover, decreasing the power consumption of the system is a matter of prime importance to allow for long-term monitoring without the need for the patient to recharge or switch batteries. Optimization of energy resources is a major concern in currently available technologies and a great effort is being made towards the development of low power consumption systems, often coming at a cost of lower precision, computational power and data transmission [15]. In the original design, each SN was connected to an AFE daughter-board, so each one of the four muscles was monitored by a separate AFE. In the new design, however, each AFE can acquire signals from more than one muscle because the ADS1298 has 8 input channels. So it is possible to connect up to 8 pairs of electrodes to each AFE. In the first prototyping phase only a set of two muscles will be monitored using a single sensor node in each limb. This allows saving resources, decreasing total power consumption and makes the system more comfortable for the user.

The circuit design recommended for EMG applications was adapted to acquire sEMG signals from two channels. For the AFE, many of the functionalities offered by the ADS1298 were not used since they are for ECG-specific applications. So, apart from the RLD channel, all the other channels that were not necessary were not being used were inactivated and therefore the correspondent conditioning circuitry was not included in the design, which considerably decreased the amount of space and energy allocation require in the PCB. Regarding circuit components, each input channel was conditioned with filters and diodes for patient safety issues and for the protection of the chip against excessive currents. Furthermore, internal reference and internal clock were chosen over external configuration, thus avoiding the use of additional components. The unused input channels were connected to the analog voltage supply through pull-up resistors, and similarly unused digital inputs were all connected to the digital voltage in the same manner. The voltage supply is 3 Volt and pull-up resistors were 10k. Additional components were included for power management. The analog channel protection includes two schottky diodes and two low pass filters with cut-off frequencies of 153 Hz and 339 Hz for high-frequency blockage. The values of the resistors were chosen to guarantee that in the case of single fail the maximum current flowing of the patient would not exceed the 500A recommended by the IEC 60601-1 norm. The use of schottky diodes was recommended in user application notes of the ADS1298. In each SN a BAS40XY SOT363 diode was used, since this package contains four diodes, thus allowing for a more compact design.

The ADS1298 datasheet suggests two different configurations for the RLD: either routing the RLD signal through the patient body using a reference electrode, or by feeding

the output signal of the RLD amplifier back into the chip multiplexer to serve as reference for the PGA of the input channels. The effects of using either configuration in this application were unknown, so a jumper was added to the circuit to allow for changing the configuration in different tests. The AFE board was conceived to interface directly with the textile leads in the leggings, whereas the main-board is mounted on top of it through connectors. The electrical contact between the AFE and the leads is guaranteed by eight small metal-plated pads pierced into the PCB. These pads will be sewed to the leggings using conductive yarn to establish a path for the current. In addition, the AFE board also contains a connector for SPI communication with the main board. The connector provides extra links to the CS, RESET and PWDN pins of the ADS1298 thus allowing for the microcontroller of the main-board to dynamically configure these pins. In order to detect eventual flaws in the circuit and correcting before sending the design to be fabricated in a local company, an intermediate version was designed. In this prototyping phase the small size packages of the electronic components were changed to larger packages, so the circuit could be fabricated in department of electrical engineering. This version uses a PGA package ADS1298. A schematic is presented in the first Figure of Annexe A. Until present date, the prototype is not yet finished, so it was not possible to conduct the proper preliminary tests.

In light of the application of the prototype in gait analysis of patients with impaired walking capabilities, it becomes essential to improve comfort, portability and autonomy of the final product. With these characteristics in mind, one of the project purposes is the development and design of a more compact, light and energy efficient SN. The miniaturized version of the sEMG AFE was designed using small scale and low-power components. To capture and digitize bio-signals, the newly developed highly integrated biosignal specific low-power, 8-channel, 24-bit AFE device ADS1298 from Texas Instruments Inc. (Dallas TX, USA) was a natural choice. This analog-to-digital converter has 24-bit resolution and offers 8 input channels for multi signal acquisition. Furthermore, it has the advantage of low power consumption (0.75mW/channel) and low input-referred noise (4VPP), as well as internal gain in the range of 0-12, which is rather important for this application. Due to size restrictions, a BGA configuration was used. The circuitry (see Figure in Annexe A). includes a conditioning circuit for the ADS1298, a digital interface with the network and a RLD circuit. The chip and the conditioning circuit were incorporated in a Printed Circuit Board (PCB), made of flexible substrate (PCV) to enhance the compactness and ergonomics of the prototype.

D. Code

A code for communication between the microcontroller in the main-board and the AFE was also developed. This code has the following functionalities: initialization of the ADS1298, data retrieval in continuous mode, reset and standby configurations. The code was written in C language to be afterwards included as a library in the main driver code of the

microcontroller. A flowchart of the implemented algorithm is presented in Annexe B

III. RESULTS

A. System Analysis and Validation

1) *Processing*: The results of the filtration are shown in Figure 3,4,5 and 6 and correspond to the sensor placed on the front of the upper limb while performing the segment A. Figure 3 and 4 corresponds to EMG filtration performed with CE and TE, respectively. Fig.1b-2b and Fig.1c-2c shows the EMG signals, after the median filter to adjust the offset and the LP to remove the noise, respectively. The obtained signal after RMS is shown in Fig.1d-2d. Inertial signals filtration is presented in Figure 5 and 6, in which is possible to visualize the results after the average and LP filter for both inertial sensors and both type of electrodes.

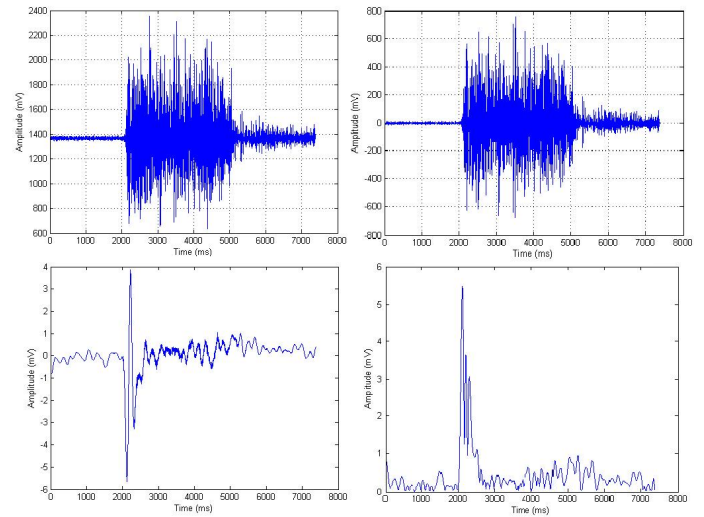


Fig. 3. EMG signal acquired in the upper limb front with segment A and CE. a) Initial EMG signal; b) EMG after average filter; c) EMG after average and LP filter; d) EMG after average, LP and RMS filter.

2) Activity Profiles identification:

• One Sensor

As represented in Fig.7 the aligned signals obtained with CE present for one peak of contraction, two peaks of acceleration and angular rotation. However, in the tests with TE the second peak is very subtle.

• Multiple sensors

Low pass filtered EMG signals for the test segment e, walking, are shown in Figure 8 for each of the 4 CE placed on the leg. Especially for the lower limb back module, we can distinguish clearly the peaks corresponding to each of the six steps performed with the right leg. As expected, the contraction pattern seems to differ according to the muscle. To compare and analyze the functional relationship between the 4 different muscles, it is necessary to align the multiple signals. Given different acquisition events (it was impossible to conduct trials at the same time with the same subject) there were no textile-conventional pairs to align.

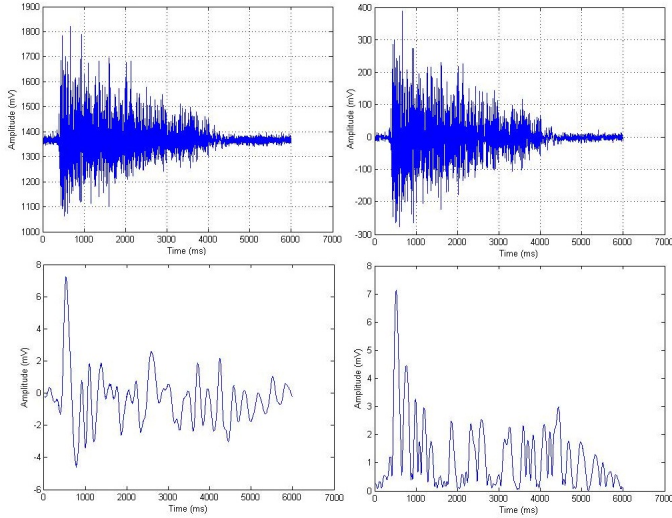


Fig. 4. EMG signal acquired in the upper limb front with segment A and TE. a) Initial EMG signal; b) EMG after average filter; c) EMG after average and LP filter; d) EMG after average, LP and RMS filter.

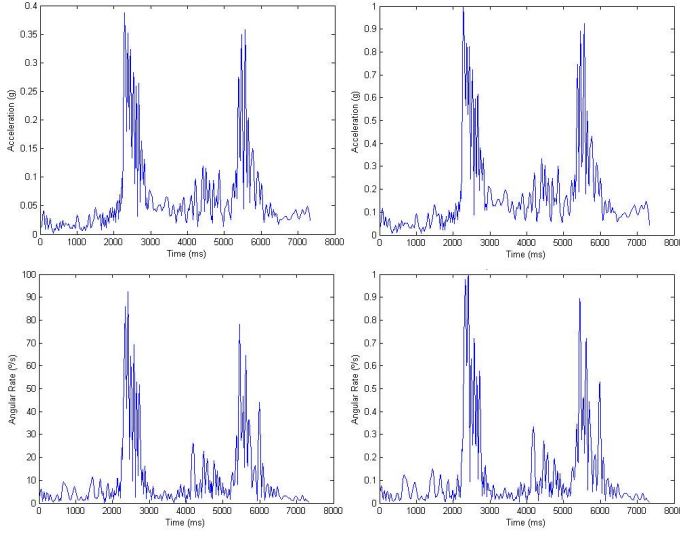


Fig. 5. Inertial signals acquired in the upper limb front with segment A and CE. a) Acceleration signal after average filter; b) Acceleration signal normalized in amplitude after average and LP filter; c) Gyroscope signal after average filter; d) Gyroscope signal normalized in amplitude after average and LP filter.

3) *Multiple Alignment*: The algorithm devised has successfully aligned all signals establishing a common time base. For instance, for signal "ContraoS1-1" shown in figure 9 it produced the following alignment matrixes:

$$D = \begin{pmatrix} 0 & -46 & 8 & -10 \\ 46 & 0 & 105 & 0 \\ -8 & -105 & 0 & -260 \\ 10 & 0 & 260 & 0 \end{pmatrix} \quad (12)$$

$$D_{avg} = \begin{pmatrix} 0 & -51.00 & 105.67 & -102.67 \\ 51 & 0 & 139.67 & 39.67 \\ -105.67 & -139.67 & 0 & -127.67 \\ 102.67 & 39.67 & 127.67 & 0 \end{pmatrix} \quad (13)$$

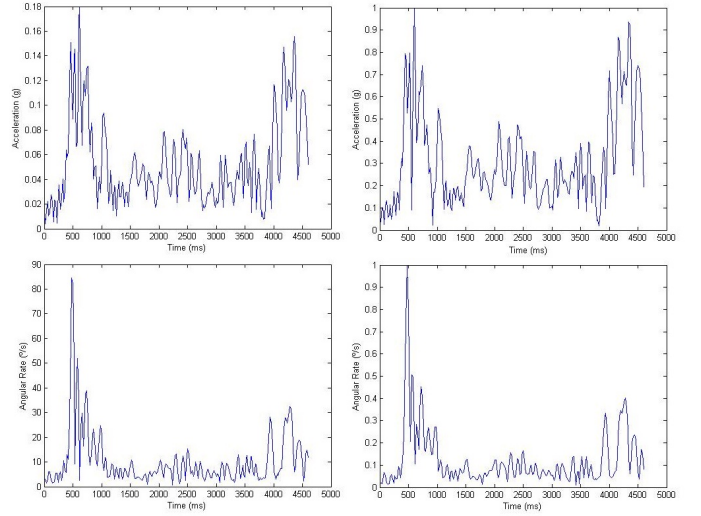


Fig. 6. Inertial signals acquired in the upper limb front with segment A and TE. a) Acceleration signal after average filter; b) Acceleration signal normalized in amplitude after average and LP filter; c) Gyroscope signal after average filter; d) Gyroscope signal normalized in amplitude after average and LP filter.

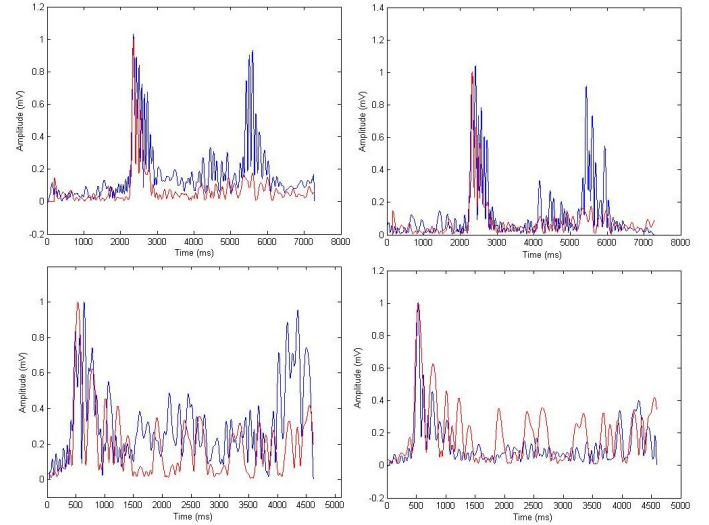


Fig. 7. Signals alignments acquired in the upper limb front with segment A. a) EMG and acceleration alignment with CE; b) EMG and gyroscope alignment with CE; c) EMG and acceleration alignment with TE; d) EMG and gyroscope alignment with TE. Blue - inertial signal; Red - EMG signal

Resulting in the following global delays:

$$d_1 = -103; d_2 = -40; d_3 = -140; d_4 = 0; \quad (14)$$

From which we can extract that 4 is our earliest signal, and by cutting d_i samples from each signal we will have a better alignment.

The resulting alignment yields the comparison of figure 10

The quality of the alignment is not subject to any parameter of performance (for the alignment itself was computed to yield the best value of cross correlations). Only by inspection can we determine that the "phase shift" like quality is lessened by the global alignment.

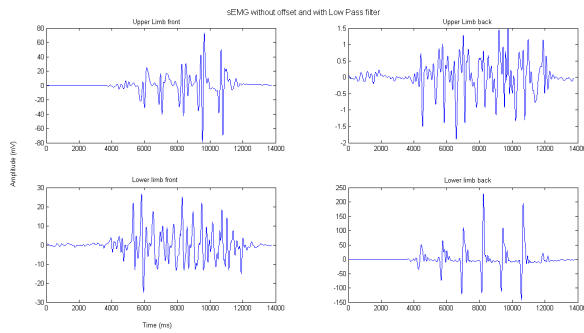


Fig. 8. EMG signal acquired in segment e with CE and filtered with the low pass filter. a) upper limb front; b) upper limb back; c) lower limb front; d) lower limb back.

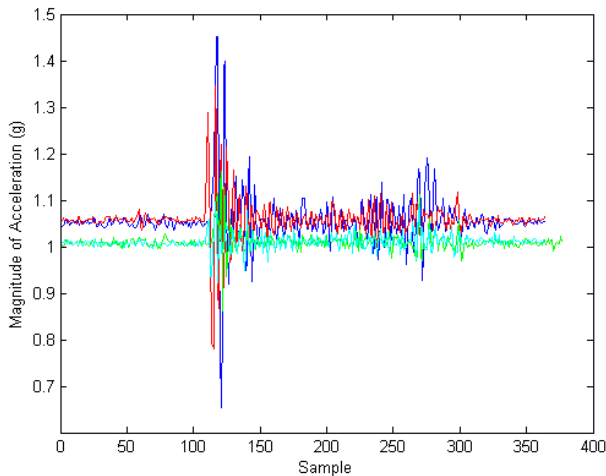


Fig. 9. Magnitude of the IMU from the 4 sensors: blue - sensor 1, red - sensor 2, green - sensor 3, cyan - sensor 4.

There can occur the problem of signal loss by temporary communication failure in the middle of the signal - generating sample time intervals for which there is no data. This, severely debilitates the alignment of the other channels, and is a vulnerability we found. However this is due to an undesirable error which is expected to be corrected in the acquisition and communication robustness.

4) *Signal to Noise Ratio*: As presented in Table I the SNR of EMG data collected with TE (mean for all tests was 1,6881) was in general lower than SNR of EMG data collected with CE (mean for all tests was 1,8334). However for the walking test the opposite was verified. This could be due to the lower stability of the TE comparing with CE when the user is walking.

Based on Table I and Figures 3 to 7 it is possible to conclude that no significant difference exists between EMG signals captured with TE and EMG signals captured with CE. In the future it will be necessary to perform the tests using TE and CE simultaneous and analyze both signals using the Bland-Altman plot in order to obtain more accurate conclusions about the difference between TE and CE EMG signals.

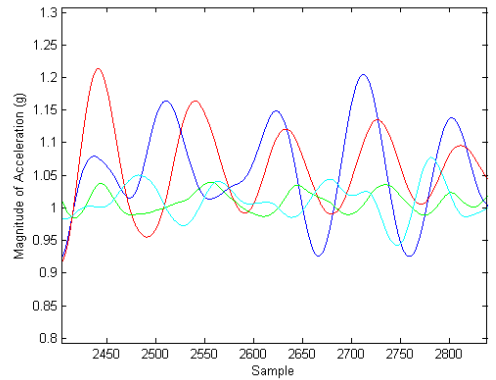
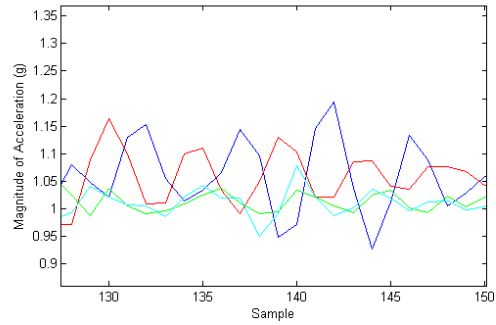


Fig. 10. Close up of some peaks from figure 9 (top) before alignment; (bottom) after alignment and resampling

TABLE I
SNR FOR CE AND TE EMG DATA, FOR DIFFERENT TESTS

	CE	TE
S1 contraction	2,6529	1,6906
S2 contraction	1,4421	1,4591
S7 contraction	1,6297	1,5048
Max contraction	1,8646	1,2823
Running	2,0015	2,0569
Walking	1,4094	2,1246

IV. DISCUSSION

The filtration of the EMG signals was successfully achieved using first an average filter to eliminate the offset, then a low pass filter reduced the noise of the signal, which permitted to obtain a better signal, finally the RMS filter highlighted the peaks of the signal improving signal alignment and comparison between different signals.

The filters applied for the inertial signals were not as successful as for the EMG. The offset was fully removed with the average filter. Noise removal proved to be more difficult with the low pass filter because the inertial signals still presented some noise after filtering, especially with TE.

Since the simultaneous usage of both sets of electrodes was not possible, the alignment and correlation of the data acquired with TE and CE for each test was unfeasible. However, the detection of locomotion activity profiles in the segments performed with CE may be useful to map some of these patterns in the data from TE and consequently, conclude if any information is lost by using TE instead of CE.

From the data acquired with one sensor in the front of upper limb, while the segment A was performed, it is possible

to observe that when the muscle contracts an acceleration and an angular rotation is promoted. After the muscle relaxation another peak of acceleration and angular rotation is observed. This second peak may correspond to the return to initial position. In the relaxation state no contraction occurs, only acceleration and rotation, which this is in accordance with the obtained graphics. When comparing the same segment with TE, the EMG and inertial signals show a similar pattern. However the second peak of gyroscope was more attenuated and the comparison was not precise since SNR for this segment was lower than with CE, as seen in the first line of the Table I.

It was not feasible to compare different tests because the amplitudes of the signals had different ranges. This was due to the recurrent changes on the gain and the loss of TE humidity with time. Despite this limitation, for the same test the acceleration has showed to be higher with more muscle contraction, which is in accordance with literature [6]. The tests with the TE and leads revealed the presence of parasitic interference in the acquired signals. In order to assess the level of noise affecting the signals, some simple motor tasks were conducted inside an anechoic camera. It was noted from the shape of the noise that it was probably caused by crosstalk between the electrode leads and the data leads. After some adjustments in the leads of the leggings, this effect was attenuated and the following tests were not affected by this noise.

A very important feature of movement analysis systems for activity monitoring and prediction, such as the case of gait analysis, is the capacity of proving real-time signal processing. That can be accomplished either by implementation processing tools on the microcontroller of the sensor node itself, or by relaying the data to a local work station where the collected data can be processed using more powerful resources.

However, the computational and power constraints imposed by the hardware used, low power microcontrollers, poses a major challenge to firmware developers. Fast and computational efficient algorithms are necessary for on-chip data processing, which many times may not be available. Another advantage of processing data in the sensor node rather than on a remote platform is that it allows for considerable data dimensionality reduction through the computation of clinically relevant parameters, which are transmitted in place of the whole collected signal. This strategy not only improves the speed of data communication in the network but also decreases the energy requirements of the system.

The method utilized here is based on getting the clock information from the node which is on the path to the BS node with minimum cost. Each node sends a request to the closest neighbor node and the receiver node replies with a message including its real time clock, so each data packet generated by the sensors has time stamping information. Therefore, this information can be used for time synchronization. There are some delays related to the propagation time (considered negligible), processing time and to the tolerance of the clock crystal. With 300 ms refreshing period, the error associated to the protocol is estimated in 18 s. The measured average processing time is about 180 s and since the EMG sampling

frequency results in a Period of 1ms, which is more than (18018) μ s, this method satisfies the timing synchronization.

Apart from this error related to the protocol, there is also an error associated with the acquisition of the signals. Each IMU sample is affected by an intrinsic delay that can reach 20ms. This delay corresponds to the time interval when the microcontroller collects the data samples to add to the packet. The precise delay varies for each sample and cannot be quantified. On the other hand, the data is streamed out of the microcontroller in a packet with 255 bytes length, each packet containing the time of first sample. The time stamp information (in the beginning of the packet) are issued by the Base Sensor Node according to its internal clock, so ideally they should be synchronized for all modules. However, due to a degree of imprecision associated with the clock, it was verified that at times there were some time lapses in signals coming from a particular SN, which could compromise the global synchronization of the signals. It was not possible to assess the maximum error that could affect the signals due to the complexity and topology of the mesh network implemented in the system. However, with the information available and from a qualitative point of view, it did not seem that both the sEMG and IMU signals were incongruent. The point was to evaluate whether there were significant delays and movement artifacts in the signals which would invalidate the system a gait analysis tool for healthcare purposes. However, it is not straightforward to conclude whether or not these small errors could translate into a diagnosis mistakes because it would depend to some extent in what kind of signal processing and classification methods would be done on the data. A future improvement in the communication protocol would be the introduction of synchronized time stamps in the signals so that an absolute alignment could be done in offline mode.

During the execution of the tests with the TE, it was necessary to wet them in order to obtain a sufficient acceptable signal. This auxiliary process is not feasible for clinical applications and is also a limitation of the actual system.

V. CONCLUSION

Taking results together, the main conclusion is that several limitations of the system itself are still to be solved. Nevertheless, important results are worth being noticed. One of the main purposes of this work was to evaluate the already available functional prototype, its performance and suggest alterations. In fact, the prototype was tested and its main limitations have been enumerated during the previous text. A miniaturization of the hardware was proposed and some problems such as the way the SN would attach to the stockings were solved.

Initially three types of tests were planned: compare the results of TE with CE and evaluate the influence of both moisture and movement artifacts in the TE signals. Ideally the first set of tests would be performed with the simultaneous acquisition of both TE and CE. In this way, correlation between signals and Bland-Altman plots would be acquired and significant differences could be assessed. Unfortunately that was not possible, but yet the performed tests allowed to infer

that despite being more attenuated than CE signals, TE and CE signals do not seem significantly different. The influence of moisture in TE signals was assessed and the movement artifacts, although have not been directly tested, were visible and their influence already discussed. Results from these tests showed that contrarily to the initial expectation, the moisture does affect TE signals but the presence of sweat is not negative. In fact moisture improves the gain of TE and besides being benefic it is necessary. Concerning the effect of stockings/TE movements, movement does affect signals. The extent in which movement artifacts degrade TE signals was not clearly assessed, but tests with the future prototype which will include the suggested alterations will answer that question. In the future, these tests must be redone with the new functional prototype. This will include our modifications and miniaturized hardware, but despite of already being ordered a few time ago, until the delivery of this report, it has not arrived.

Further considerations about the evaluated prototype are described next. We identify the impossibility to wash the stockings, which is not feasible for multiple users or even for long-term monitoring because of transpiration. Besides, we discovered that according to the normatives, the wearable devices should be replaced each three months. Based on that, stockings should be disposable and a new configuration should consider this problem. The actual system is also not completely practical due to the attaches connecting the nodes to the stockings. Concerning the execution of the planned tests, the system should be more stable during running or jumping in order to obtain less noisy signals, the acquisition of EMG signals simultaneously with TE and CE is mandatory in order to obtain more feasible results. Therefore future work should focus on the improvement and optimization of the system, to reduce the identified limitations, and a few suggestions are presented in the next section.

VI. FUTURE WORK

Further testing is necessary to validate the system and prove its reliability. Future tests should acquire TE signals using the miniaturized solution that was designed. The circuit and TE for the next prototype must be directly embedded into the stocking cloth and not manually stitched, as it was done for the current prototype. The solution of manually stitching the attaches to the stockings with conductive wire still has to be reviewed. Better alternatives to attach them efficiently to the cloth were still not found. On a later stage, conductive wiring in the cloth should be electrically isolated, for instance, covering them with insulator material. For that purpose, different solutions have to be tested, as for example silicones or resins. A silicone circle could also be placed around the TE in order to prevent electrode dislocation. Future tests, with an advanced model of the prototype, should also use the segments already specified but performed initially by healthy test subjects and then by persons with special conditions, such as Parkinson patients or injured athletes. Tests concerning movement artifacts must be done, and in order to do so we suggest to acquire signals of the each segment with TE dislocated few centimeters from

the optimal point and compare the obtained signals. Another important issue that should be addressed is the reliability of the data, that is, lossless transmission of the signals. In healthcare applications this point is of particular relevance since medical diagnosis is based on the quantitative parameters extracted from the physiological data. So, the loss of a segment of signal due to transmission failure is not acceptable. A future improvement in the communication protocol would be the introduction of synchronized time stamps in the signals so that an absolute alignment could be done in offline.

ACKNOWLEDGMENTS

The authors would like to thank Ruben Dias for his participation as team supporter and adviser.

REFERENCES

- [1] J. Tan. *Advancing clinical gait analysis through technology and policy*. PhD thesis, Massachusetts Institute of Technology, 2009.
- [2] H. Stolze, S. Klebe, C. Baecker, C. Zechlin, L. Friege, S. Pohle, and G. Deuschl. Prevalence of gait disorders in hospitalized neurological patients. *Movement disorders*, 20(1):89–94, 2004.
- [3] W. Tao, T. Liu, R. Zheng, and H. Feng. Gait analysis using wearable sensors. *Sensors*, 12(2):2255–2283, 2012.
- [4] A. Peppe, C. Chiavalon, P. Pasqualetti, D. Crovato, and C. Caltagirone. Does gait analysis quantify motor rehabilitation efficacy in parkinson's disease patients? *Gait & posture*, 26(3):452–462, 2007.
- [5] M. Ferrarin, L. Lopiano, M. Rizzone, M. Lanotte, B. Bergamasco, M. Recalcati, and A. Pedotti. Quantitative analysis of gait in parkinson's disease: a pilot study on the effects of bilateral sub-thalamic stimulation. *Gait & posture*, 16(2):135–148, 2002.
- [6] A. Galajdová, D. Šimšík, and L. Madarász. Possibilities of gait parameters prediction from emg data by neural networks. In *Computational intelligence: Proceedings of the 3rd international symposium of Hungarian researchers: Budapest*, pages 159–164, 2002.
- [7] R.W. Bohannon and A. Williams Andrews. Normal walking speed: a descriptive meta-analysis. *Physiotherapy*, 97(3):182–189, 2011.
- [8] C.M. Yang, C.M. Chou, J.S. Hu, S.H. Hung, C.H. Yang, C.C. Wu, M.Y. Hsu, and T.L. Yang. A wireless gait analysis system by digital textile sensors. In *Engineering in Medicine and Biology Society, 2009. EMBC 2009. Annual International Conference of the IEEE*, pages 7256–7260. IEEE, 2009.
- [9] F. Derogarian, R. Dias, C. Ferreira, and M.G. Tavares. Using a wired body area network for locomotion data acquisition. In *Electromyography*.
- [10] A. Zambrano, F. Derogarian, R. Dias, M.J. Abreu, A. Catarino, A.M. Rocha, S.J. Machado, F.J. Canas, T.V. Grade, and C.M. Velhote. A wearable sensor network for human locomotion data capture. In *PHealth 2012: Proceedings of the 9th International Conference on Wearable Micro and Nano Technologies for Personalized Health*, page 216. IOS Press, 2012.
- [11] M. Silva, A. Catarino, H. Carvalho, A. Rocha, J. Monteiro, and G. Montagna. Study of vital sign monitoring with textile sensors in swimming pool environment. In *Industrial Electronics, 2009. IECON'09. 35th Annual Conference of IEEE*, pages 4426–4431. IEEE, 2009.
- [12] S.H. Nawab, S.S. Chang, and C.J. De Luca. High-yield decomposition of surface emg signals. *Clinical Neurophysiology*, 121(10):1602–1615, 2010.
- [13] Jee Hong Quach. *Surface electromyography: Use, design & technological overview*. University of Concordia, 2007.
- [14] T.O. Mera, D.E. Filipkowski, D.E. Riley, C.M. Whitney, B.L. Walter, S.A. Gunzler, and J.P. Giuffrida. Quantitative analysis of gait and balance response to deep brain stimulation in parkinson's disease. *Gait & Posture*, 2012.
- [15] S. Patel, K. Lorincz, R. Hughes, N. Huggins, J. Growdon, D. Standaert, M. Akay, J. Dy, M. Welsh, and P. Bonato. Monitoring motor fluctuations in patients with parkinson's disease using wearable sensors. *Information Technology in Biomedicine, IEEE Transactions on*, 13(6):864–873, 2009.

APPENDIX A ENLARGED SCHEMATIC DETAIL

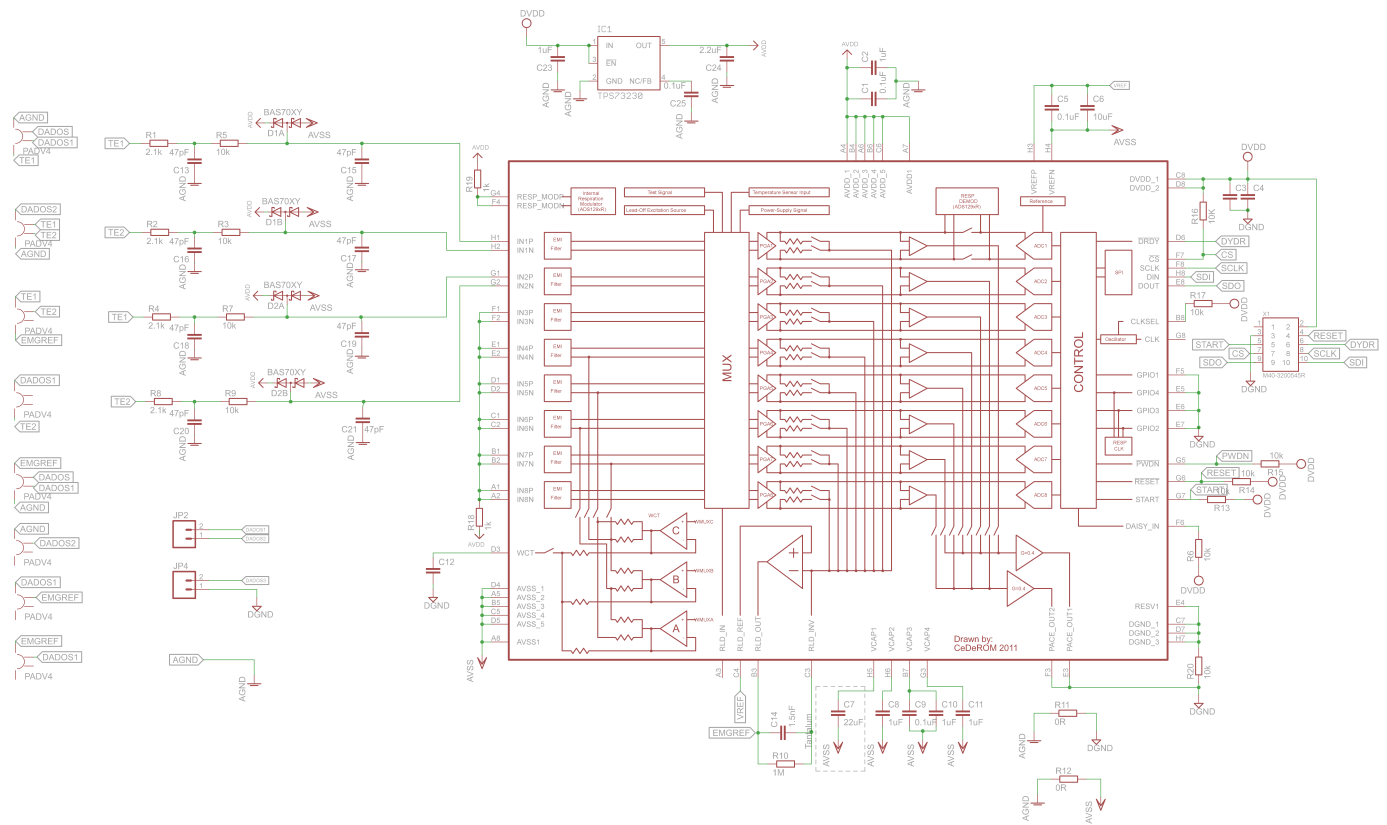


Fig. 11. Circuit schematic of the miniaturized Analog Front End, using an ADS1298 with BGA package and reduced-size components.

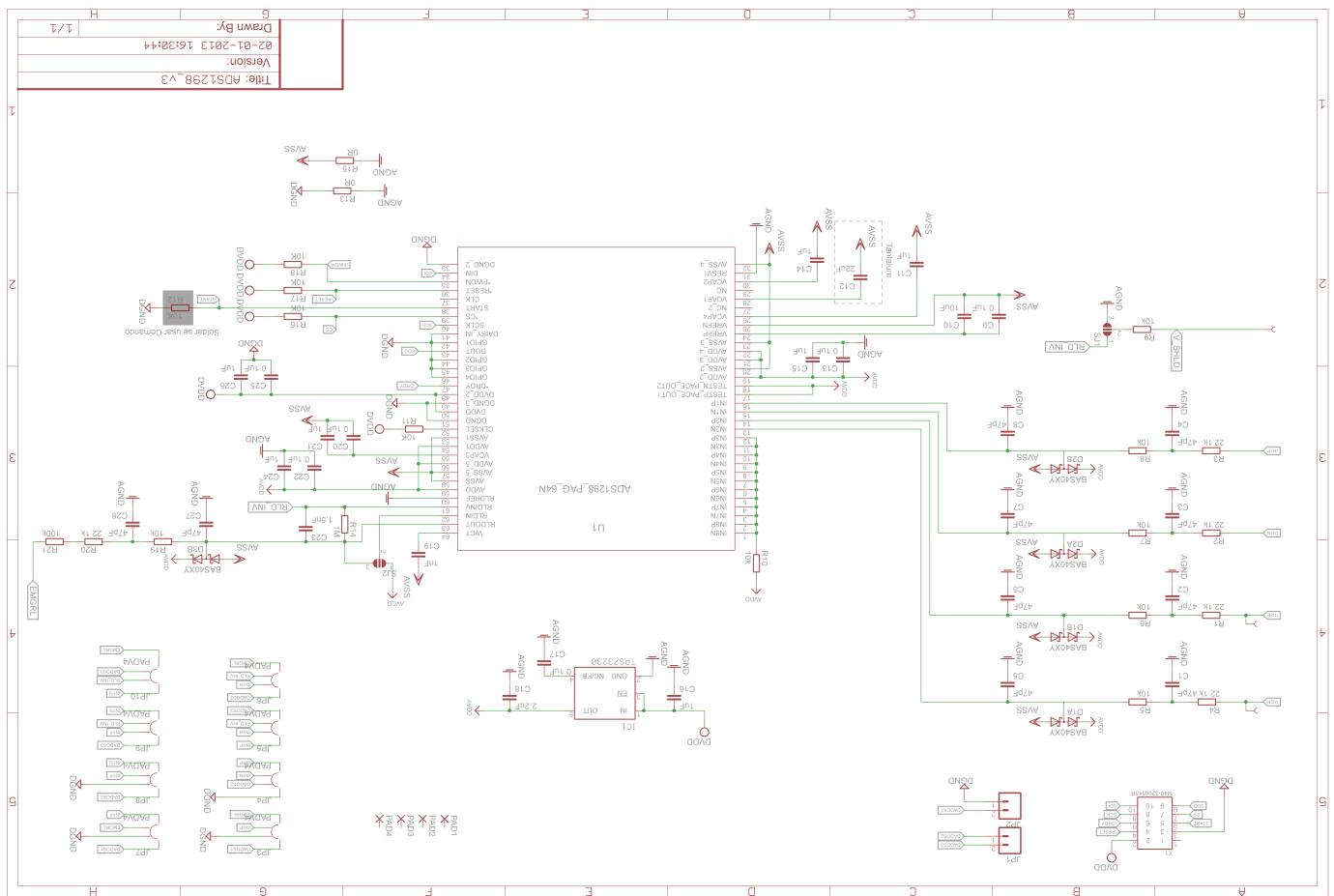


Fig. 12. Circuit schematic of the intermediate miniaturized Analog Front End prototype, using an ADS1298 with PGA package, for preliminary tests.

APPENDIX B
IMPLEMENTED CODE

